Cell Transplantation
Volume 34: 1–15

DOI: 10.1177/09636897251323351
journals.sagepub.com/home/cll
Sage

Robot-Assisted Stereotactic Microinjection Method for Precision Cell Transplantation in Rat and Canine Models

Deqiang Han[1], Sichang Chen[2], Yuan Wang[1], Xueyao Wang[1], Xingzhe Wang[1], Tianqi Zheng[1], and Zhiguo Chen[1,3,4]

Abstract

Cell transplantation is a promising approach for addressing neurodegenerative conditions. In this study, we developed a robot-assisted stereotactic microinjection system for transplanting cells. We evaluated the factors that affect cellular graft viability and other properties, including the gauge of the syringe needle and the injection rate. We systematically compared the synchronous withdrawal injection (SWI) and fixed-point injection (FPI) procedures in agarose and rat brain models. *In vitro* assessments revealed superior dye dispersion with SWI compared to FPI, and *in vivo* analyses confirmed that SWI reduced the tissue injury and improved cell distribution in the striatum. We applied this robot-assisted technique to evaluate the accuracy and safety of cell transplantation in canine models. Overall, this strategy enhances the accuracy and safety of graft delivery, potentially improving outcomes and advancing therapeutic strategies for the clinical treatment of neurodegenerative disorders.

Keywords

cell transplantation, robot-assisted stereotactic microinjection, central nervous system, neurodegenerative disease

[1]Cell Therapy Center, Beijing Municipal Geriatric Medical Research Center, National Clinical Research Center for Geriatric Diseases, and Key Laboratory of Neurodegenerative Diseases, Ministry of Education, Xuanwu Hospital Capital Medical University, Beijing, China
[2]Department of Neurosurgery, Xuanwu Hospital Capital Medical University, Beijing, China
[3]Center of Neural Injury and Repair, Beijing Institute for Brain Disorders, Beijing, China
[4]Center of Parkinson's Disease, Beijing Institute for Brain Disorders, Beijing, China

Submitted: January 15, 2025. Revised: February 8, 2025. Accepted: February 10, 2025.

Corresponding Author:
Zhiguo Chen, Cell Therapy Center, Beijing Municipal Geriatric Medical Research Center, National Clinical Research Center for Geriatric Diseases, and Key Laboratory of Neurodegenerative Diseases, Ministry of Education, Xuanwu Hospital Capital Medical University, Beijing 100053, China
Email: chenzhiguo@gmail.com

Graphical Abstract

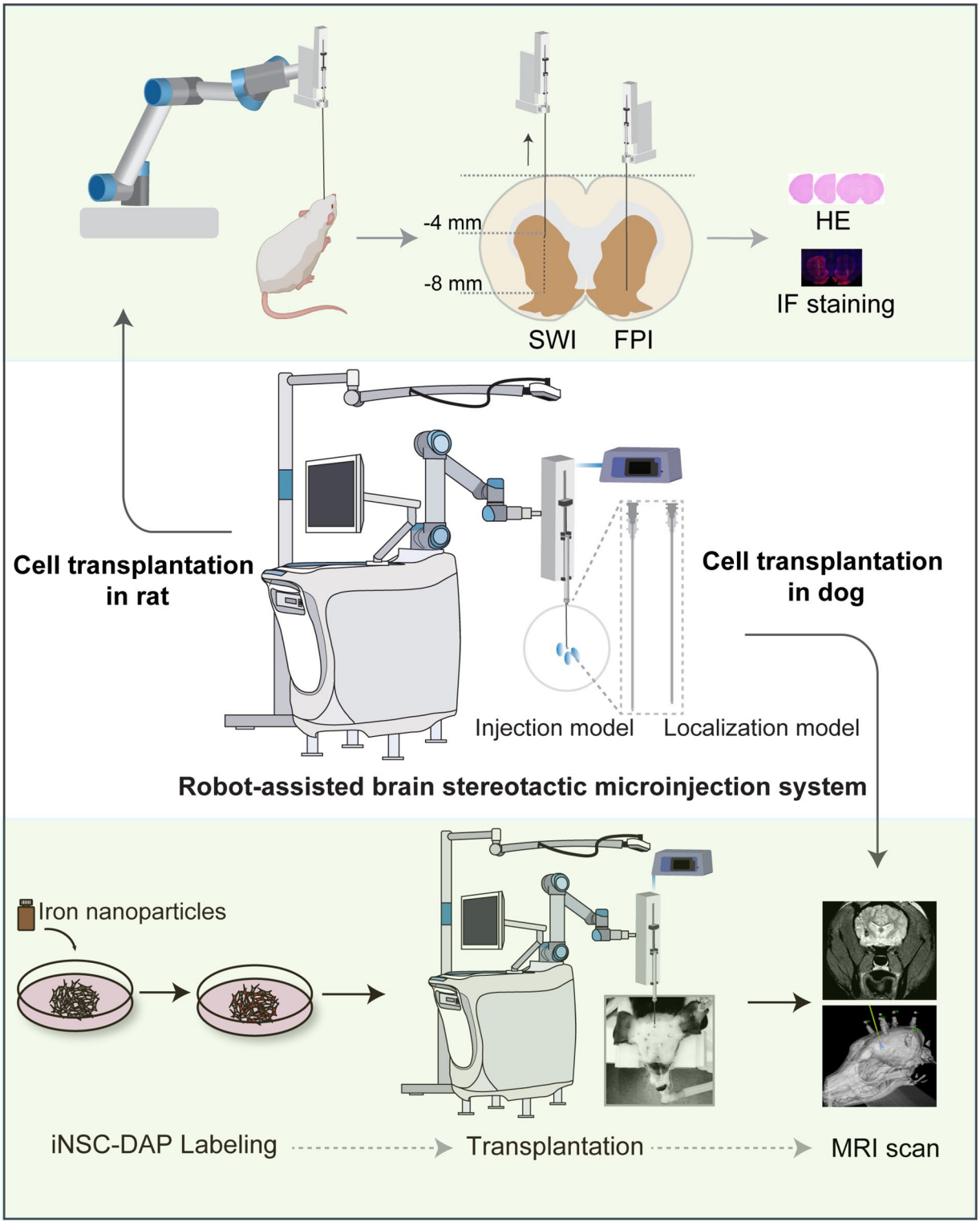

Introduction

Cell transplantation is an effective strategy for treating neurodegenerative diseases, including Parkinson's disease (PD), Alzheimer's disease, spinal cord injuries, and stroke, and has been clinically applied for neurorestorative treatments of those diseases in recent years[1–7]. However, the central nervous system (CNS) is mechanically and physiologically delicate, with even minor injuries leading to tissue damage and severe neurological deficits. Therefore, delivery methods for specific areas of the nervous system must be precise while minimizing tissue trauma[8].

Several delivery methods have been investigated to address these challenges. Intranasal delivery uses unique pathways connecting the nasal cavity to the CNS to offer a noninvasive means of administering stem cells to the brain[9]. Similarly, lumbar puncture allows stem cells to circulate through the cerebrospinal fluid, reaching the brain and the spinal cord[10]. Although these noninvasive techniques generally cause less damage than direct injections or surgical interventions, they lack the precision required for effectively targeting specific injury sites. Direct injection into the brain or spinal cord parenchyma is generally more effective in ensuring the successful replacement and integration of transplanted cells into damaged tissues[11].

Frame-based stereotactic injections, which are widely used for brain biopsy procedures, facilitate highly precise cell delivery to targeted brain regions[12]. However, this technique involves the use of a rigid frame that stabilizes the head of the patient and ensures accurate alignment with the target area in brain. The process is cumbersome and may increase the discomfort for the patient[13].

The robot-assisted stereotactic frameless guidance system integrates high-resolution imaging technologies to facilitate different types of neurosurgical interventions, including stereotactic biopsy, deep brain stimulation (DBS), and tumor resection[14]. For example, the ROSA and Neuromate robots assist surgeons in planning and performing complex brain surgeries with enhanced precision and efficiency[15]. This system facilitates precise navigation through the complex anatomy of the brain, allowing surgeons to target specific regions in the brain with minimal deviation. It improves the efficacy of the procedure and patient outcomes.

Given the advantages of surgical navigation robots and the need for precise cell injections, a dedicated brain localization system for microinjections needs to be developed. However, studies on robot-assisted systems designed and optimized for stereotactic injections are rare. To address this issue, we developed a novel robot-assisted stereotactic microinjection method specifically designed for cell transplantation and validated its effectiveness in rat and canine models. Our findings suggested that this system is a promising approach to advancing cell transplantation in the context of neurodegenerative conditions. By addressing challenges related to precision and safety, this technology can improve treatment strategies and patient outcomes.

Materials and Methods

Cell Culture and Preparation

Neural stem cells with eGFP knock-in (eGFP-iNSCs) were cultured following methods described in another study[16]. The culture medium comprised 48% DMEM/F12 (Gibco, 11330-032) and 48% Neurobasal-A (Gibco, 10888-022), along with 1% each of B27 (Gibco, 17504044), N2 (Thermo Fisher, 17502048), NEAA (Gibco, 11140-050), and GlutaMax (Gibco, 35050-061). In addition, the medium contained 10 ng/ml hrLIF (Millipore, LIF1010), 3 μM CHIR99021 (Gene Operation, 04-0004), and 2 μM SB431542 (Gene Operation, 04-0010). For the differentiation of eGFP-iNSCs into dopaminergic progenitors (eGFP-iNSC-DAPs), the cells were first dissociated into single units using Accutase (Invitrogen, A11105-01). These single cells were then plated at a density of 200,000 cells per well in six-well plates coated with PDL and laminin. The differentiation commenced with phase I of the DA differentiation medium, which included 96% DMEM/F12 (Gibco, 11320-033), 1% each of B27 (Gibco, 17504044), N2 (Thermo Fisher, 17502048), NEAA (Gibco, 11140-050), and GlutaMax (Gibco, 35050-061), along with 1 μM SAG1 (Enzo, ALX-270-426-M01) and 100 ng/ml FGF8 (Peprotech, 100-25) for the first 10 days. Next, phase II of the DA differentiation medium was used for the rest of the differentiation process; it consisted of 96% DMEM/F12 (Gibco, 11320–033), 1% each of B27 (Gibco, 17504044), N2 (Thermo Fisher, 17502048), NEAA (Gibco, 11140-050), and GlutaMax (Gibco, 35050-061), along with 10 ng/ml BDNF (Peprotech, 450-02), 10 ng/ml GDNF (Peprotech, 450-10), 1 ng/ml TGF-βIII (Peprotech, 100-36E), 10 μM DAPT (Sigma-Aldrich, D5942), 0.2 mM ascorbic acid (Sigma-Aldrich, 1043003), and 0.5 mM cAMP (Sigma-Aldrich, D0627).

Animals

Healthy male Sprague-Dawley rats (230–250 g, 8–10 weeks old, n = 12) were used for graft injection. These specific pathogen-free (SPF) rats were purchased from Vital River (Beijing, China, license No. SCXK (Jing) 2021–0006) and kept in a controlled environment with temperatures maintained between 22°C and 25°C and relative humidity at 50%–65%. They were housed in pairs in cages under a 12-h/12-h light/dark cycle and with continuous access to food and water. The rats used in the experiments were naïve, and no drug testing was conducted. In addition, one adult male dog weighing 8.5 kg was included in the canine model experiment. This dog was housed alone in a cage and purchased from the Sharing Institute of Biological Resources (Beijing, China; license No. SCXK (Jing) 2020–0009). All

animal experiments adhered to the guidelines set forth by the Chinese Ministry of Public Health, as well as applicable national and international regulations. The procedures involving animals received approval from the Animal Ethics Committee (rat approval number: XW-20210423–2; dog approval number: XEX20230609).

Cell Viability Analysis

We used various custom needles to evaluate cell viability during transplantation. Induced neural stem cell-derived dopaminergic progenitors (iNSC-DAPs) were prepared in a sterile cell suspension medium Lactated Ringer's solution (Yaowang Pharm, H20057482). The cells were loaded into sterile syringes fitted with custom needles, and different injection rates were evaluated using a programmable syringe pump. After injection, cell viability was assessed using a hemocytometer (SmartCell 800, Monwei). This procedure was performed in triplicate (n = 3) to enhance reliability. By comparing cell viability across different needle diameters and injection rates, we identified the optimal conditions that maximize cell survival during transplantation.

Agarose Test

To illustrate the process of intracerebral injection *in vitro*, a solution containing 0.25% Trypan blue (Beyotime Biotech, ST2780) mixed with 30% glycerol (Sigma-Aldrich, G5516) in saline was introduced into 0.8% agarose (YEASEN, 11208ES60). An overall volume of 30 µl was administered at a rate of 3–5 µl/min using either the SWI or FPI. Sequential images were captured at various time intervals throughout the injection process.

MIRB Nanoparticle and iNSC-DAP Labeling

Molday ION Rhodamine B (MIRB), a suspension of iron-based superparamagnetic nanoparticles, was purchased from BioPhysics Assay Laboratory (CL-50Q02-6A-50). Cells labeled with MIRB can be visualized by magnetic resonance imaging (MRI). To label iNSC-DAPs, 20 µg Fe/ml MIRB was added to the iNSC-DAP culture medium and incubated for 18–20 h. Following labeling, the cells were harvested by dissociating them into single cells using Accutase, followed by centrifugation at 250 × *g* for 5 min. The resulting cell suspension was prepared for implantation, achieving a final concentration of 1.0×10^5 cells/µl.

Robot-Assisted Stereotactic Microinjection

All surgical instruments underwent standard sterilization procedures prior to use. The experimental animals underwent preoperative MRI incorporating T1-weighted three-dimensional (3D) gadolinium-enhanced sequences and additional sequences. For computed tomography (CT) spatial registration, titanium fiducial markers were surgically implanted under general anesthesia to establish cranial reference points. CT scans (1 mm slice thickness) were acquired in prone positioning, with subsequent removal of fiducial markers post-transplantation.

For surgical planning and registration, imaging datasets (MRI and CT) were integrated into Remebot robotic navigation platform (RM-200; Baihui Weikang Tech.). The animal was under general anesthesia, cephalic fixation was achieved in appropriate position. The marker-based registration was performed with subsequent validation through two test markers to ensure targeting accuracy. A precision craniotomy was created at the predetermined entry coordinate.

For cell transplantation, the fixation structure was installed and secured in place, the microinjection unit was preinstalled, and the setup was marked with a sterile marker pen. After registration and navigation localization, the guide cannula in localization model was inserted into the target area. The microsyringe was connected to the needle, air was expelled, and the cell suspension was aspirated. The microsyringe was loaded into the microinjection pump unit in the correct position. The injection was started at a rate of 3 µl/min for 10 min, and the solution was withdrawn slowly at 0.5–1 mm/min. Following the injection, the needle was kept in place for 8 min before retraction (either manually or using the robotic system). Finally, the wound was disinfected and sutured. After the operation, MRI was conducted to monitor the status of the transplantation.

Frame Stereotaxic Brain Injections

For frame stereotaxic injections, all rats were anesthetized via an intraperitoneal injection of a mixture containing 25 mg/ml ketamine, 1.3 g/ml xylazine, and 0.25 mg/ml acepromazine (2 ml/kg). Each rat was injected with 4 µl of cell suspension on each side. The left striatum was targeted via SWI, whereas the right striatum received FPI. For SWI, the target coordinates for the right corpus striatum were anteroposterior = 0.8 mm, lateral = 2.7 mm, and vertical = −8 mm, with a withdrawal range of 4 mm; for FPI, the target coordinates were anteroposterior = 0.8 mm, lateral = −2.7 mm, and vertical = −8 mm. After the experiments ended, the rats were euthanized by administering sodium pentobarbital, following the AVMA Guidelines for the Euthanasia of Animals (2020 Edition).

Immunofluorescence Staining

For cell culture staining, iNSC-DAPs were grown on coverslips coated with poly-D-lysine (PDL) and laminin, followed by fixation with 4% paraformaldehyde (PFA) for 10 min. The cells were subsequently washed twice with phosphate-buffered saline (PBS) (5 min per wash). This was followed by blocking with 3% donkey serum containing 0.3% Triton X-100 in PBS (PBST) for 1 h at room temperature. Primary

antibodies were applied overnight at 4°C in a solution of 1% donkey serum with 0.3% PBST, after which the sections were incubated with secondary antibodies for 1 h in the same blocking solution. Finally, the cells were stained with 4',6-diamidino-2-phenylindole (DAPI) for 15 min at room temperature.

For IF analysis of brain slices, rats were perfused with saline and 4% PFA, after which the brains were dissected and immersed in a 30% sucrose solution for dehydration. Frozen sections (40-μm-thick) were produced using a freezing microtome and stored in TCS buffer (consisting of 25% glycerin, 30% ethylene glycol, 5 mM sodium-phosphate buffer) at 4°C. The brain slices were washed twice with PBS (5 min per wash), followed by blocking with 3% donkey serum containing 0.3% PBST for 2 h at room temperature. Then, the samples were incubated overnight with primary antibodies in 1% donkey serum with 0.3% PBST at 4°C. The following day, the slices were treated with secondary antibodies for 2 h in the same solution and stained with DAPI for 15 min at room temperature.

Histological Analysis

The collected tissues were fixed in 4% PFA for 48 h, embedded in an optimal cutting temperature (OCT) compound, and stored at −80°C. The OCT-embedded frozen tissue was cut into slices (20-μm-thick). Adjacent tissue sections were stained with H&E (Beyotime, Shanghai, China) for general observation. Images are captured using a Pannoramic scanner (3DHISTECH, Budapest, Hungary). The distribution profile of quantitative immunofluorescence (IF) was analyzed using the plot profile tool in ImageJ.

Statistical Analysis

The data were expressed as the mean ± SD and analyzed using GraphPad Prism 9.0. The differences among and between groups were determined by paired *t*-tests and one-way analysis of variance (ANOVA), followed by Bonferroni's multiple comparisons post hoc test. Statistical significance for all differences was determined $P < 0.05$.

Results

Establishment of a Novel Robot-Assisted Brain Stereotactic Microinjection System for Cell Transplantation

To achieve more accurate and safer therapeutic cell delivery, we established a novel robot-assisted brain stereotactic system for microinjection that can be used for cell therapy or gene therapy. This system consists of a robot-assisted stereotactic surgery device, a microinjection pump, an adaptor, microinjection unit with a needle set (Fig. 1). The robot-assisted surgical device was developed to help surgeons perform delicate and precise surgical procedures, particularly in the field of neural system surgery. Although robot-assisted surgery technology is extensively used in clinical settings[14], its application in cell transplantation remains rare. In this study, we used the Remebot robotic system[17], which includes a planning system, a videometric tracking system, and an operating arm equipped with specialized software. This setup facilitates precise and controlled movements throughout the transplantation process. The microinjection pump helps deliver a precise volume of cell suspension into the targeted area of the brain with accuracy and uniformity. To ensure that the connection was secure and leak-proof, we designed the adaptor to serve as a connector between the robotic arms of the robot-assisted stereotactic surgery device and the microinjection unit (including the syringe or needle), facilitating connection and precise positioning during transplantation. The microinjection unit including the syringe and customized needle sets which were designed to contain and deliver the cell suspension to the targeted brain area. The needle suite consists of three components, including a solid trocar, an outer cannula, and an injection needle (Fig. 1B). In the localization model, the solid trocar is initially inserted into the cannula and secured in place using the positioning limiter of the robotic system to lock it at the target area. In the injection model, once the target is identified, the trocar is withdrawn, and the injection needle is inserted to initiate the injection process (Fig. 1C). This approach ensures precise and controlled delivery of the cells, minimizing trauma to surrounding tissues and strengthening the integration of transplanted cells in the brain microenvironment.

Optimizing Injection Parameters for Custom Needles in Cell Therapy

We developed various types of needles tailored for cell microtransplantation. The specifications of these needles are detailed in Supplemental Table S1. The device setup is driven by an injection pump and includes parameters such as the injection rate, volume, and duration (Fig. 2A). The customized needle sets, designed for targeting the brain, are approximately19 cm long. To evaluate the impact of needle size and injection rate on cell viability during the injection process, iNSC-DAPs were loaded into syringes and injected through custom needle cannulas at various rates. The inner diameter of the customized needles ranged from 1.0 ± 0.1 mm to 1.6 ± 0.1 mm, with the injection rates varying from 3 to 30 μl/min (Fig. 2A). We observed that higher injection rates result in a more significant difference in cell viability before and after injection. Smaller needles showed greater variability in cell viability post-injection and caused increased stress and damage at higher rates (Fig. 2B). Normally, cells injected through larger-diameter needles have greater viability, suggesting less cellular trauma[18]. However, larger needles may cause greater damage to surrounding brain tissue, necessitating a balance between needle

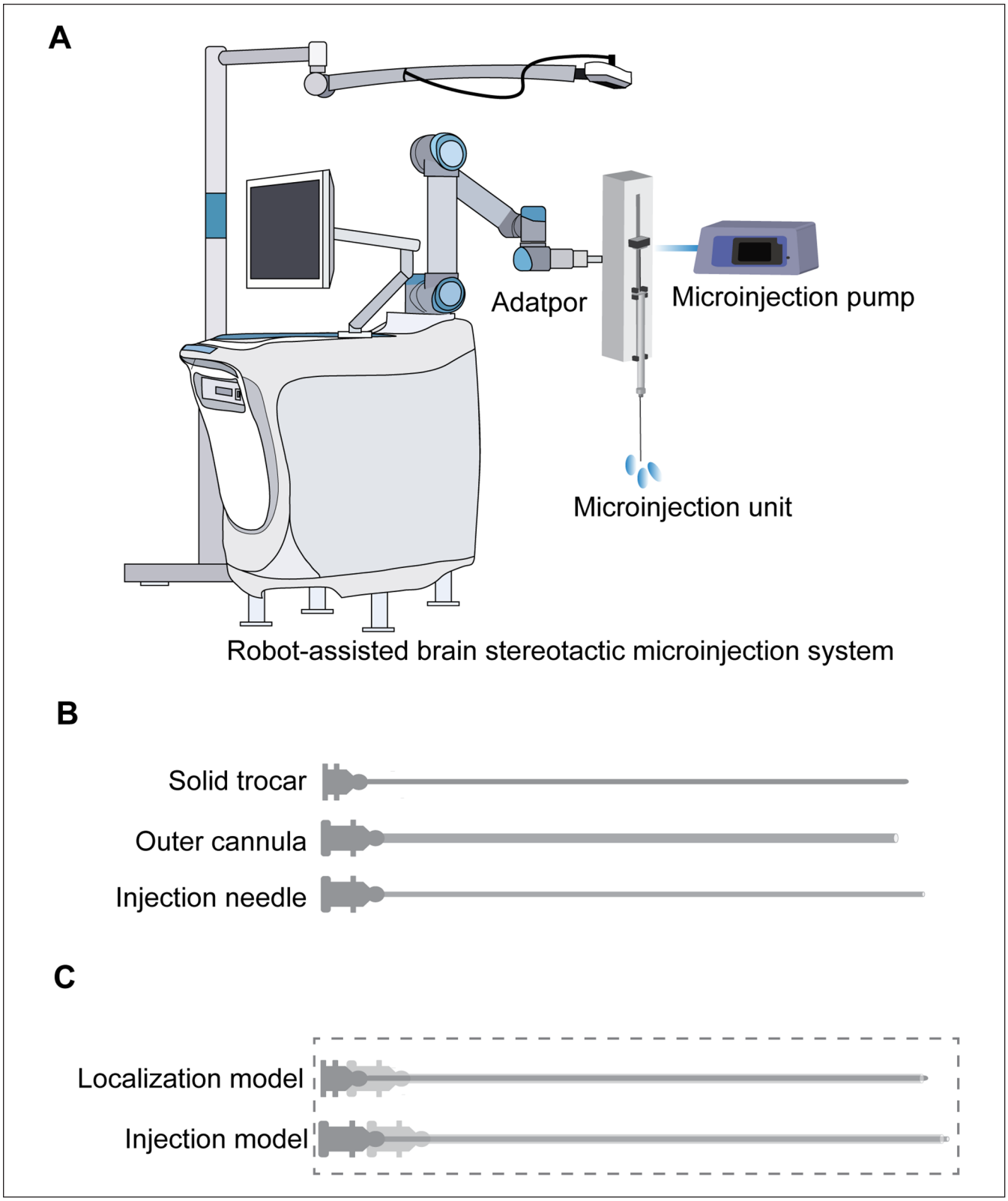

Figure 1. Establishment of a novel robot-assisted brain stereotactic microinjection system for cell transplantation. (A). Schematic representation of the robot-assisted brain stereotactic microinjection system. (B). Components of the custom injection needle suite. The needle suite consisted of three components: a solid trocar, an outer cannula, and an injection needle. (C). Two injection models of the injection needle suite were constructed. In the localization model, the solid trocar was initially inserted into the cannula and secured in place using the robotic system's positioning limiter to lock it at the target site. In the injection model, once the target was identified, the trocar was gradually withdrawn, and the injection needle was inserted to commence the injection process.

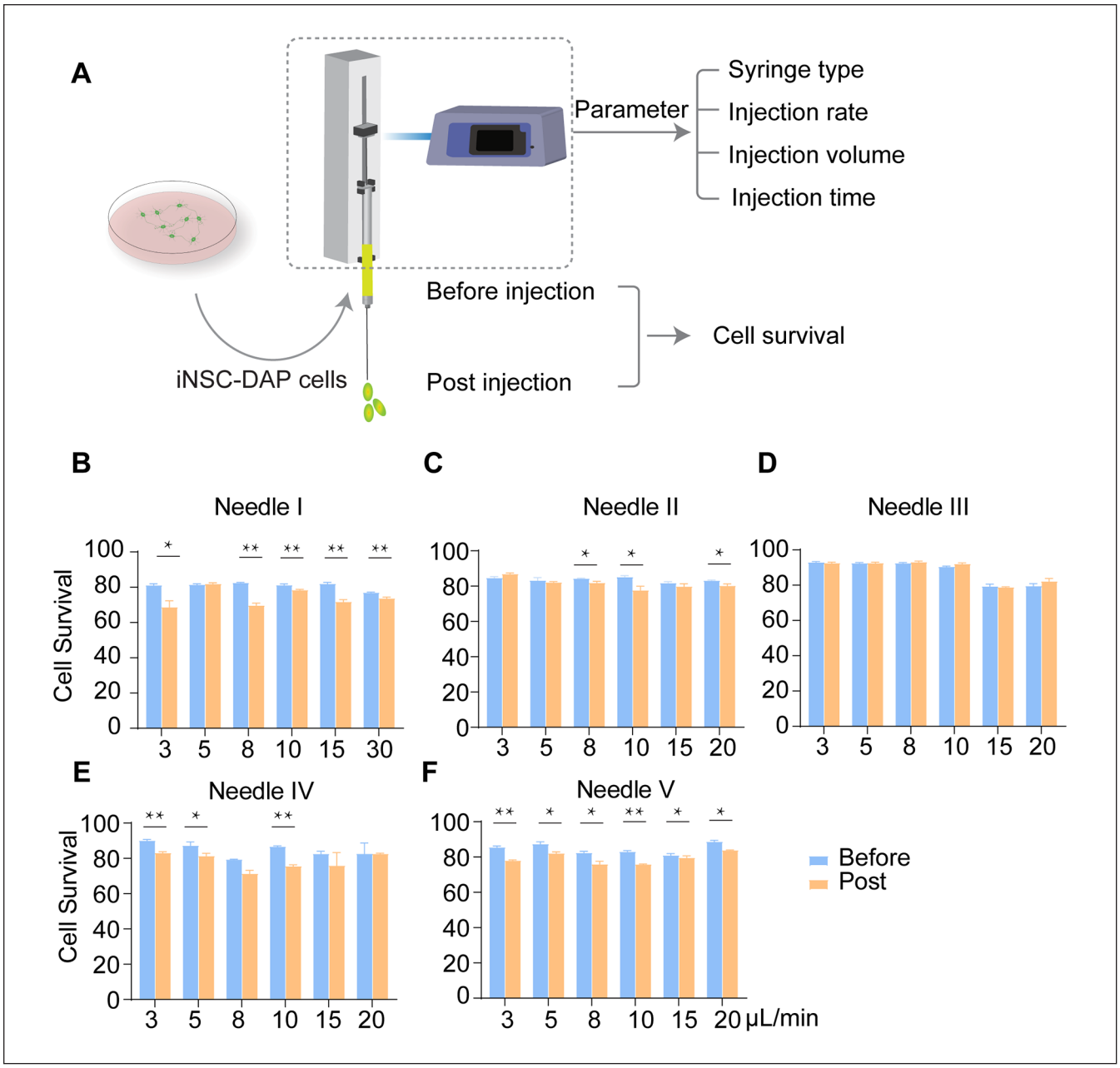

Figure 2. Optimization of injection parameters for custom needles in cell therapy. (A) Schematic representation of the device setup for iNSC-DAP injection through custom needle cannulas at various rates using an injection pump. (B-F) Cell viability of Needle I (B), Needle II (C), Needle III (D), Needle IV (E), and Needle V (F) before and after injection through custom needle cannulas. The results of cell viability are presented as the mean ± standard deviation (SD) (n = 3). Asterisks indicate significant differences between measurements taken before and after passing through the needle. * $P < 0.05$; ** $P < 0.01$.

size and cell viability. For example, Needle III, which has an inner diameter of 0.6 ± 0.1 mm and an outer diameter of 1.0 ± 0.1 mm, demonstrated a cell viability of 92.93 ± 0.42% before injection and 92.57 ± 0.51% after injection, resulting in a preinjection viability of 99.61% (Fig. 2B). This needle size maintained relatively stable cell viability, with an optimal injection rate of 3–10 µl/min. This finding highlighted that compared with faster rates, slower injection rates are associated with greater cell viability. It is suggested that the injection needle diameter and injection rate affect cell viability during cell injection procedures.

Comparison Between SWI and FPI Methods in Vitro

To assess microinjection techniques for cell delivery in the brain, we compared two methods: synchronous withdrawal injection (SWI) and fixed-point injection (FPI). SWI is a

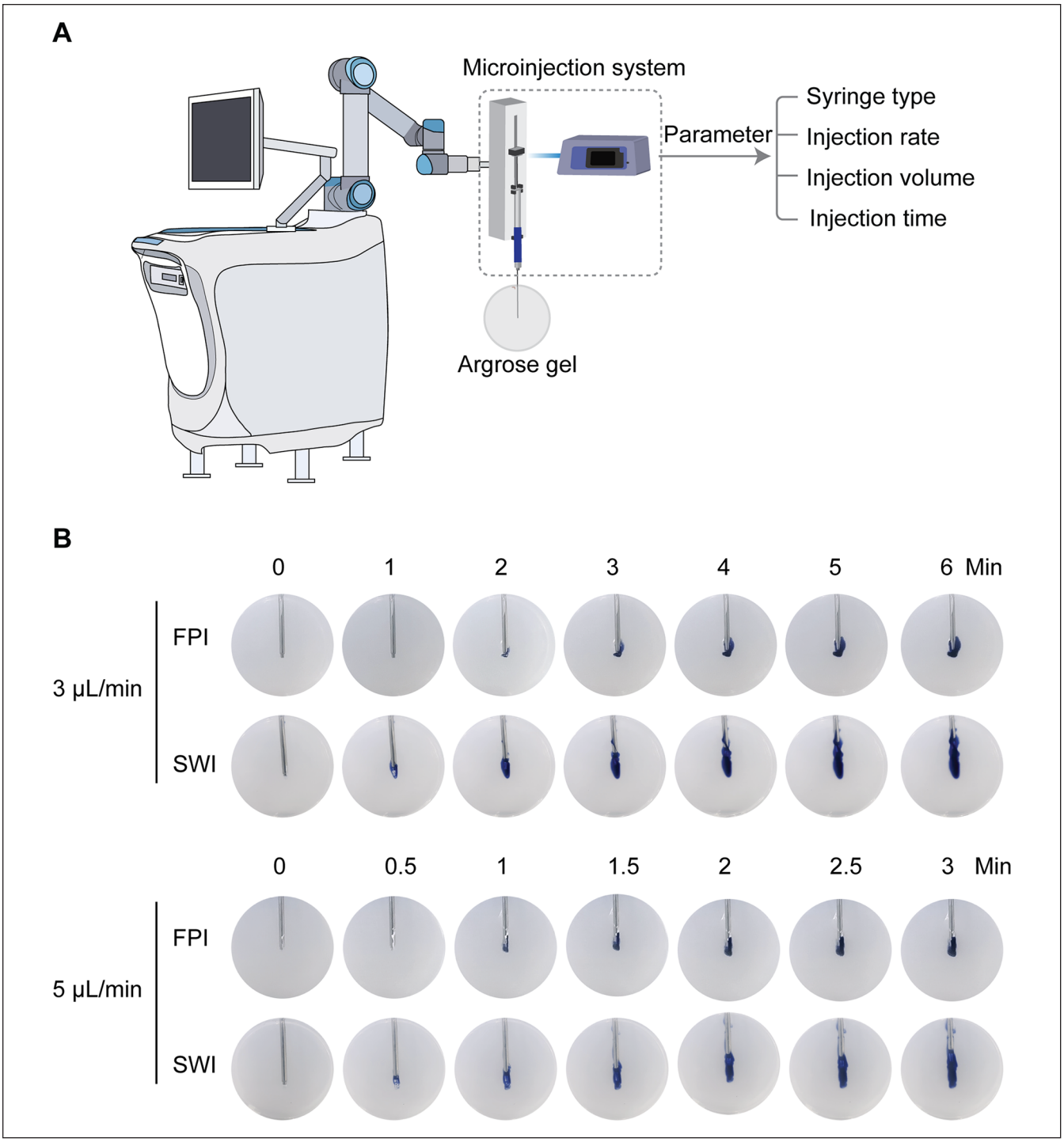

Figure 3. Comparison of SWI and FPI methods *in vitro*. (A) Schematic representation of the robot-assisted brain stereotactic microinjection system for gel injection. (B) Comparison of the SWI and FPI methods for injecting Trypan blue in agarose. In total, 30 μl of glycerol or Trypan blue solution in saline was injected at rates of 3 μl/min and 5 μl/min through Needle III. Successive images demonstrate a more even distribution of materials with SWI. SWI: synchronous withdrawal injection; FPI: fixed-point injection.

dynamic injection procedure in which the infusion of cell suspension is synchronized with the gradual withdrawal of the injection needle. FPI involves static delivery at a predefined stereotaxic coordinate, with the injection needle remaining stationary throughout the infusion process. Using the brain stereotaxic system, we injected 30 μl of 0.25% trypan blue in saline into 0.8% agarose disks using both methods at various rates (Fig. 3A). The SWI method achieved a

more uniform dye distribution throughout the agarose matrix than the FPI method. Imaging data confirmed that SWI provided enhanced spatial distribution and more homogeneous dye dispersion in the matrix (Fig. 3B). These findings suggested that SWI is better at achieving efficient dye distribution in agarose matrices, thus benefiting applications that require precise delivery.

SWI Is Superior to FPI in Vivo

To further evaluate the effect of different injection methods on tissue damage and cell distribution, we conducted frame-based stereotactic injections with iNSC-DAPs into the rat brain using the SWI and FPI methods through needles with a fitted size. For the SWI procedure, the injury needle withdrawal ranged from −8 mm to −4 mm to ensure uniform penetration through the striatal region (Fig. 4A). Histological analysis of coronal brain sections stained with hematoxylin and eosin (H&E) indicated that SWI caused significantly less tissue damage than FPI, which was associated with small vacuoles and localized damage (Fig. 4B). IF staining showed that SWI resulted in a more uniform distribution of cells in the striatum, whereas FPI resulted in less consistent cell dispersion (Fig. 4C, D, E). These findings suggested that SWI can more effectively minimize brain damage and provide a more homogeneous distribution of transplanted cells, making it a preferred method for cell transplantation in preclinical studies.

Validation of Robot-Assisted Stereotactic Microinjection for GRAFT Transplantation in Rats

To compare the effects of the SWI and FPI methods on graft transplantation *in vivo*, we conducted robot-assisted stereotactic microinjection into the rat brain using both procedures (Fig. 5A). For SWI, we used a traditional injection system with customed needle, performing injections with a withdrawal range from −8 mm to −4 mm from the skull. This method ensured consistent penetration throughout the striatal region. Histological analysis of coronal brain sections stained with H&E revealed that the SWI method led to less tissue damage than the FPI method. The FPI method resulted in the formation of small tissue vacuoles and localized damage (Fig. 5B, C). IF staining showed that cells injected via SWI were more evenly distributed throughout the striatum compared with those injected via FPI (Fig. 5D). These results indicated that SWI can more effectively decrease brain damage and achieve a more uniform distribution of transplanted cells than FPI.

Robot-Assisted Stereotactic Microinjection via SWI for Graft Transplantation in a Canine Model

To establish and validate an accurate and effective method for robot-assisted stereotactic microinjection for cell transplantation in preclinical models, we conducted cell transplantation in a canine model (Fig. 6A). Initially, for *in vivo* visualization of the distribution of the transplanted cells, we labeled iNSC-DAP cells (Supplemental Fig. S1) with a nanoiron reagent, which is detectable via MRI[19]. We first assessed the labeling efficacy by transplanting 200,000 nanoiron-labeled iNSC-DAP cells into a rat model, which is sufficient for MRI visualization (Supplemental Fig. S2). The integration of MRI and CT imaging with the Remebot robotic system facilitated precise trajectory planning and surgical execution. Preoperative MRI, which included a T1-weighted 3D gadolinium-enhanced sequence, and CT scans with a slice thickness of 1 mm ensured that the target area was accurately localized (Fig. 6B).

During the injection procedure, the cell suspension was delivered at a controlled rate of 3 μl/min over 10 min, with a synchronous withdrawal rate of 0.5–1 mm/min. The syringe and needle were held in position for 8 min postinjection to ensure optimal cell deposition. Postoperative MR scans showed the correct placement of the grafts, revealing the expected distribution with minimal artifacts (Fig. 6C, D). This method was highly reproducible, indicating its potential for reliable graft transplantation in canine models. The 3D reconstruction of the brain postinjection showed that the cells were evenly distributed (Fig. 6E). This study advanced the field of cell transplantation by offering a comprehensive and validated approach for targeted cell delivery in a large animal model. The robot-assisted stereotactic microinjection procedure is a precise and efficacious technique, and it has significant implications for translational research and clinical applications.

Discussion

In this study, we developed a novel robot-assisted stereotactic microinjection system, integrating a Remebot robot-assisted stereotactic surgery device, a microinjection pump, an adaptor, and the microinjection unit with a needle set. This system can significantly increase accuracy and decrease tissue trauma during cell delivery to the CNS. The system showed that SWI significantly outperforms FPI by providing more uniform dye distribution *in vitro*, thus reducing tissue damage while improving cell distribution *in vivo*.

Validation in rat and canine models confirmed the efficacy of the microinjection system and highlighted its ability to advance cell transplantation therapy. This phenomenon is particularly significant for neurodegenerative conditions, such as PD, in which accurate cell placement in critical brain regions, including the substantia nigra and striatum, is essential for achieving efficacious therapy and minimizing damage to the surrounding brain tissue[2,5,20]. iNSC-DAPs specifically differentiated into dopaminergic neurons have been employed to restore dopaminergic function in preclinical research and a clinical trial, which represents a promising approach to cell therapy for this condition[16,21,22].

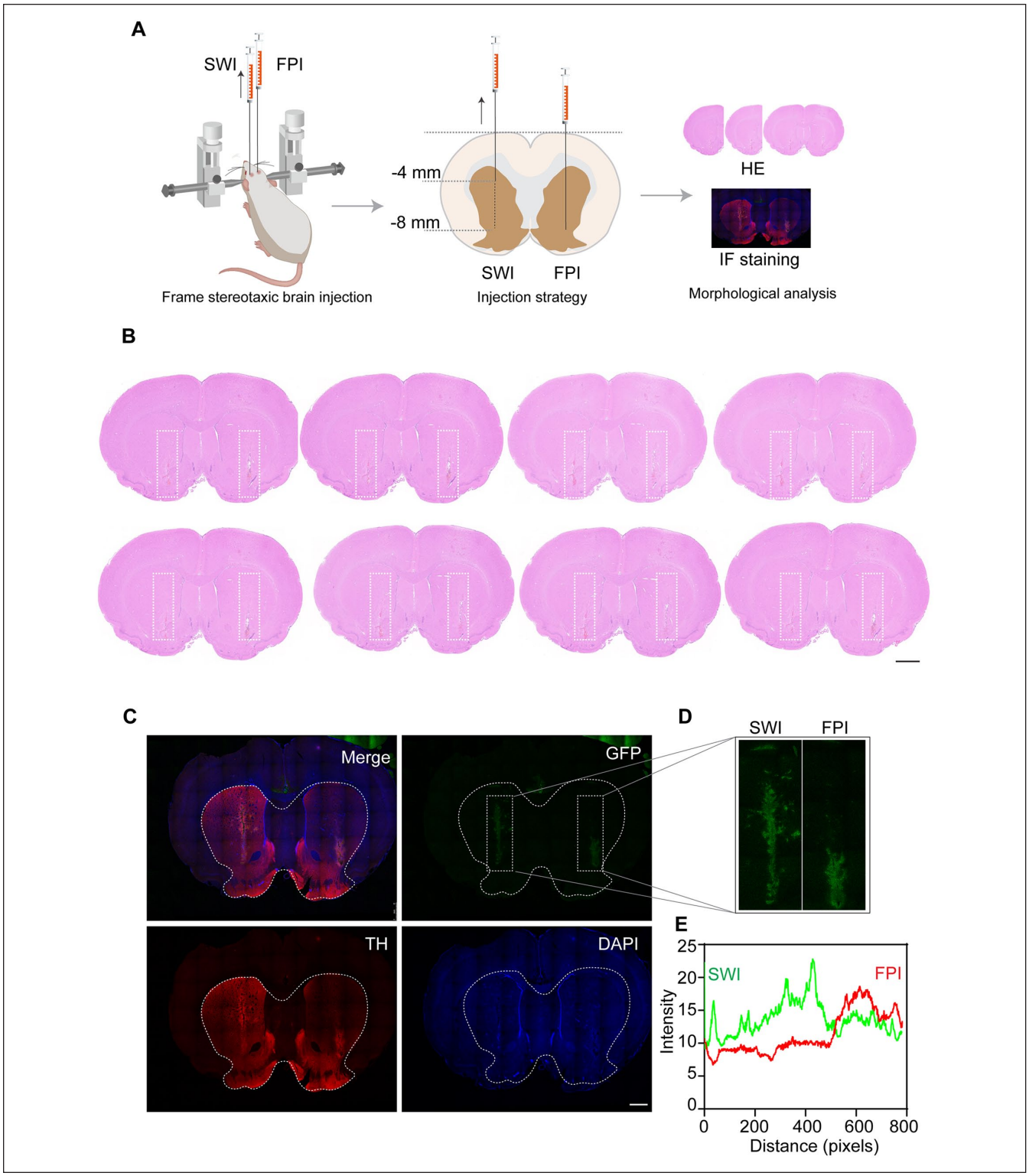

Figure 4. Comparison of SWI and FPI methods *in vivo*. (A) Schematic representation of frame-based brain stereotactic microinjection in rats using SWI and FPI methods. (B) Histologic examination of post-transplantation operations via H&E staining; scale bar: 100 μm. (C) Immunofluorescence images of graft eGFP knock-in iNSC-DAPs in the brain sections of rats using SWI and FPI methods; scale bar: 100 μm. (D) Immunofluorescence images of grafted iNSC-DAPs in rat brain sections following stereotactic injection via SWI and FPI methods, comparing the distribution and localization of transplanted cells along the needle tract. (E) Quantitative profile analysis of immunofluorescence distribution comparing SWI (green line) and FPI (red line) methods. SWI: synchronous withdrawal injection; FPI: fixed-point injection; iNSC-DAPs: induced neural stem cell–derived dopaminergic precursor cells; TH: tyrosine hydroxylase.

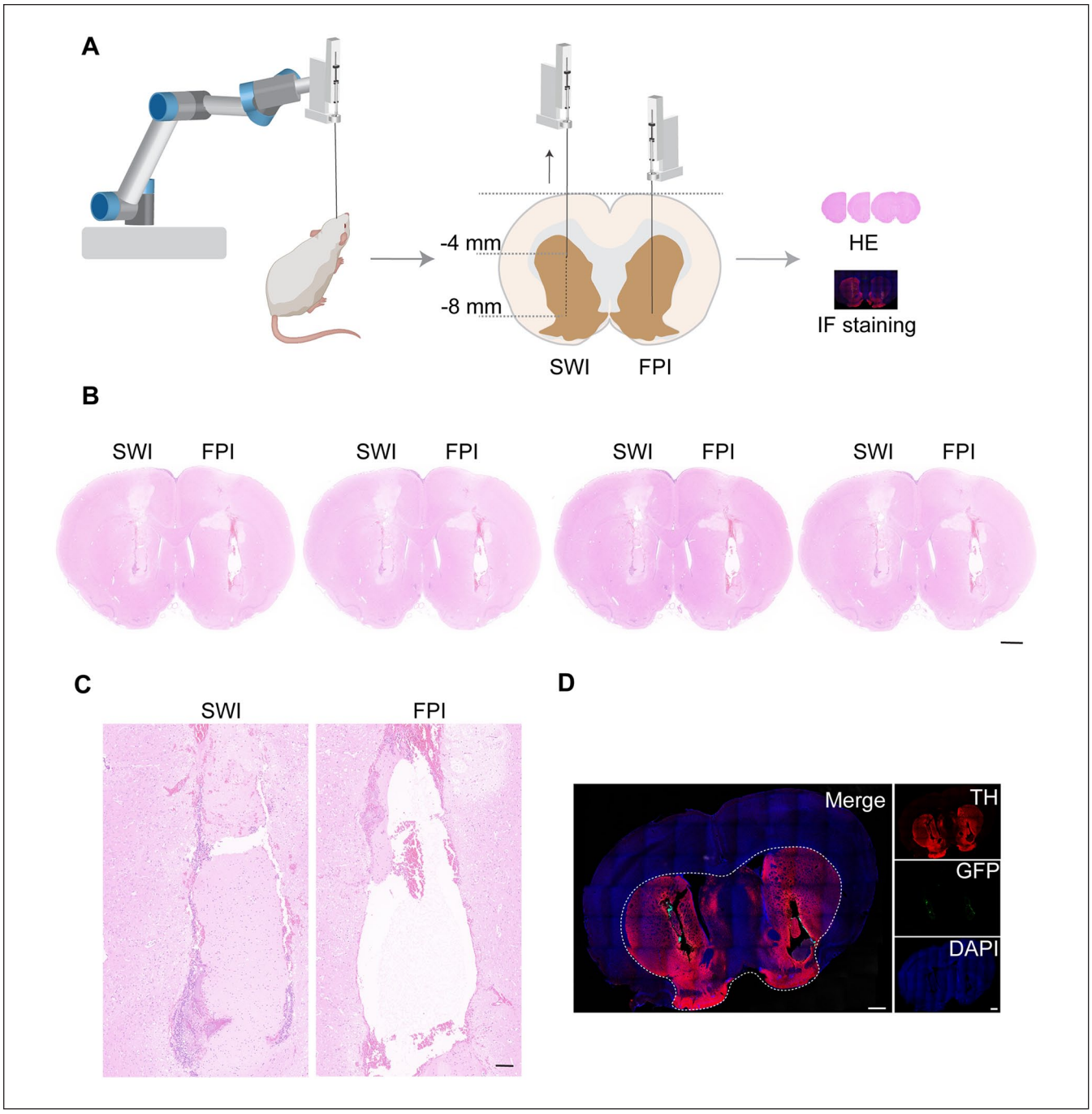

Figure 5. Validation of robot-assisted stereotactic microinjection for graft transplantation in rats. (A) Schematic representation of the robot-assisted brain stereotactic microinjection system for rats. (B) Histologic examination of post-transplantation operations via H&E staining with successive images. Scale bar: 100 μm. (C) Assessment of needle tract tissue morphology following SWI and FPI stereotactic cell transplantation by H&E staining. Scale bar: 10 μm. (D) Immunofluorescence images of graft eGFP knock-in iNSC-DAPs in the brain sections of rats. Scale bar: 100 μm. SWI: synchronous withdrawal injection; FPI: fixed-point injection; TH: tyrosine hydroxylase.

Transplanted cells subjected to intracranial injection differ significantly from those subjected to traditional chemical drugs and are more susceptible to damage, which affects their viability and effectiveness. Cellular treatments are highly sensitive to shear and pressure forces, particularly during passage through microsyringes and thin needles[18,23]. The viability of cell-based therapeutic techniques can be influenced by factors such as syringe needle size, injection rate, needle length, and the injection procedures used[18,24]. In this study, we compared the outer diameter of needles

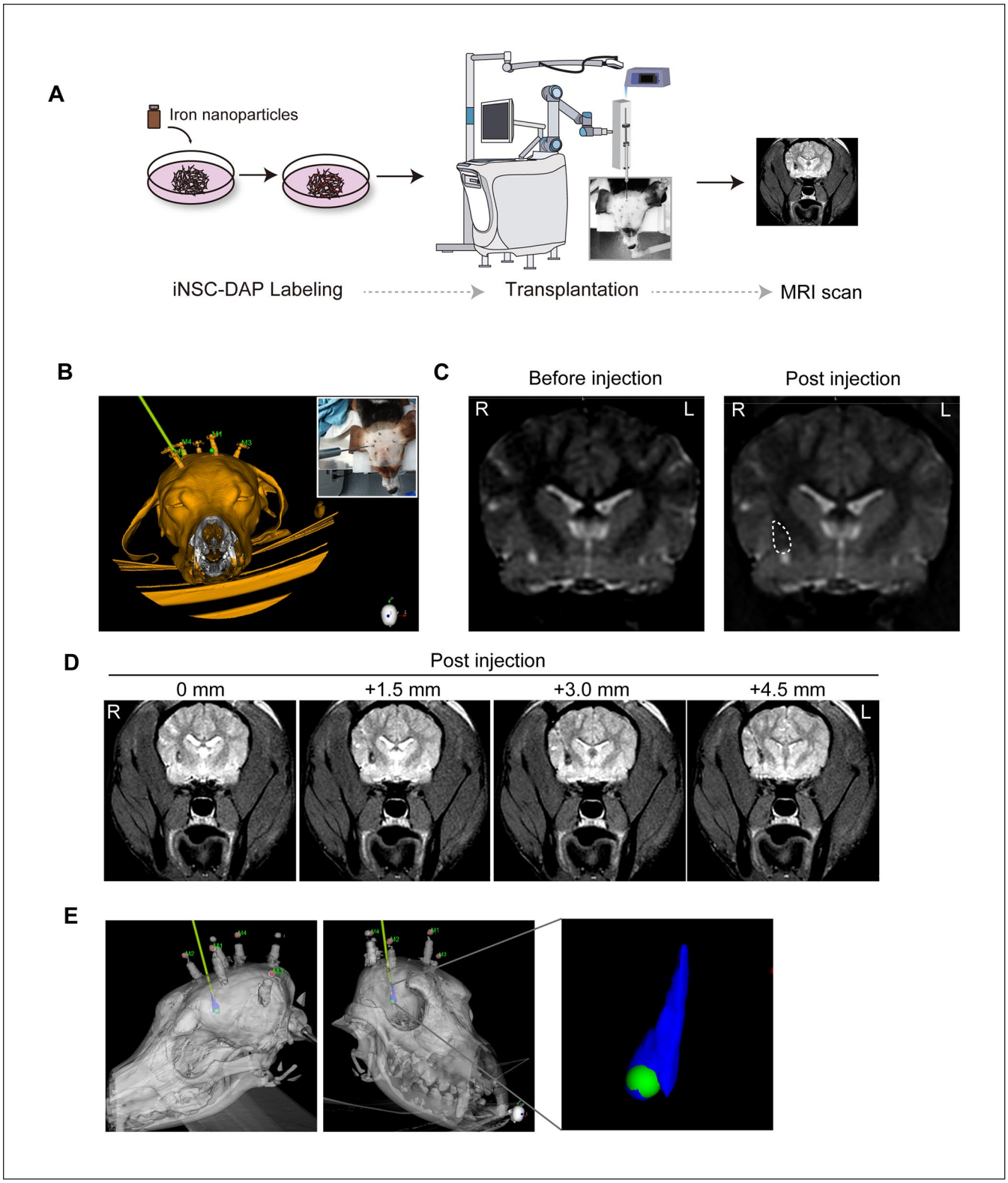

Figure 6. Robot-assisted stereotactic microinjection is conducted via SWI for graft transplantation in a canine model. (A) Schematic representation of the robot-assisted brain stereotactic microinjection system for dogs. (B) The 3D reconstruction of the injection plan according to the fusion of MRI and CT images. (C) MRI with a T1 sequence in the axial view before and after transplantation. (D) MRI T2 sequence in the axial view after transplantation. (E) The 3D reconstruction of the brain postinjection showed that the cells were evenly distributed. MRI: magnetic resonance imaging; CT: computed tomography.

ranging from 1.0 ± 0.1 mm to 1.6 ± 0.1 mm in gauge. When the needle diameter exceeds that of the cells, the shear forces exerted on the cells are relatively minimal; we found similar patterns in our study. Thus, both the needle length and injection speed are critical parameters. We evaluated injection rates ranging from 3 to 30 μl/min, and our findings indicated that higher rates may increase tissue damage and decrease cell survival. This finding indicated the need to optimize injection speeds to balance efficiency with cell integrity. Clinically, an injection rate between 3 and 5 μl/min is optimal for maintaining cell viability and minimizing adverse effects. Our *in vitro* studies using gel models supported these conclusions, demonstrating that injection rates of 3 and 5 μl/min are superior for preserving cell function.

Regarding the injection procedures, we investigated two microinjection techniques, including SWI and FPI, to assess their efficacy in cell delivery in brain research applications. Using a brain stereotaxic system, we examined these methods by injecting trypan blue into 0.8% agarose disks at different rates. Our results indicated that SWI achieved significantly more uniform dye dispersion throughout the agarose matrix. This enhanced dispersion is critical for applications requiring precise and uniform delivery of substances in complex matrices, such as brain tissue. The results of the gel assay indicated that direct injection by the FPI method frequently presents challenges, including potential blockage of the injection tube by the gel[25]. Schweitzer and Song developed a columnar injection technique designed to reduce damage to host tissue and produce a column of graft material with a greater surface area than traditional injection techniques[26]. In our experimental setup, we used a two-stage approach consisting of a localization model and an injection model. The localization model was initially used to accurately position the needle in the target region. Specifically, a solid trocar was inserted into the cannula and secured with the positioning limiter of the robotic system, which ensured accurate placement at the target location. After accurately locating the target, the trocar was withdrawn, and the injection needle was inserted to initiate SWI. This approach ensured that the injection was conducted with precision and control, thereby minimizing the risk of trauma to adjacent tissues and promoting the integration of the injected dye or cells into the brain microenvironment.

Our results showed significant differences in cell distribution and tissue damage between the SWI and FPI techniques. SWI, a process in which withdrawal and injection are performed simultaneously, offers advantages by reducing localized pressure and tissue damage, thus promoting a more uniform distribution of cells. This is particularly relevant for conditions such as PD, where a large number of dopamine-producing cells are lost and where target areas such as the striatum (including the putamen) are often extensive. Positron emission tomography (PET) imaging data indicate that accurate and homogeneous cell placement is essential for achieving efficacious therapy. The SWI approach, characterized by a decrease in local pressure and an increase in cell distribution, aligns with this requirement and decreases the adverse effects associated with FPI, which may increase local pressure and damage to brain tissues and transplanted cells. Stereotactic surgery relies on precise spatial targeting in the brain, utilizing coordinate systems to guide interventions while minimizing disruption to surrounding tissues. The robot-assisted microinjection system designed in this study is potentially compatible with different types of surgical robots. Our findings supported the potential of the system; however, using this system in clinical settings necessitates further validation through clinical trials and compliance with medical device regulations.

In this study, we achieved a significant advancement in cell transplantation technology by introducing a more precise and less invasive method for delivering cells. This technique increases the effectiveness of cell-based therapy for various neurological conditions. Clinical trials are necessary to comprehensively assess whether the system is effective and safe for humans. Successful validation in animal models paves the way for future clinical trials, translating these innovations into better treatment options for patients.

Limitations

This study focused primarily on validating the microinjection method in a non-PD animal model, limiting the generalizability of the findings to PD-specific contexts. Future studies are warranted to investigate the effectiveness of this method in PD models. In addition, the small sample size has limited the generalizability and statistical power of the results. We also focused on verifying injection precision in canine models without comparing the SWI and FPI techniques, which may have provided a more nuanced understanding of the efficacy of the method. In addition, the study did not address the variability in human anatomy, scalability, or adaptability associated with clinical applications. Long-term outcomes and potential side effects need to be comprehensively evaluated to ascertain the clinical utility of the method.

Research Ethics and Patient Consent

All the experimental procedures were conducted in compliance with the Guidelines for the Care and Use of Laboratory Animals established by the Beijing Association for Laboratory Animal Science and the National Institutes of Health Guide for the Care and Use of Laboratory Animals. All procedures performed in studies involving animals were approved by the Laboratory Animal Ethics Committee of Xuanwu Hospital Capital Medical University. For the rodent experiments, approval number XW-20210423–2 was used. The approval title is Cell Therapy for Central Nervous System Diseases. Date of approval: April 23, 2021. For dogs,

approval number XEX20230609 was used. The approval title is "Study on brain stereotactic cell transplantation." Date of approval: June 9, 2023.

Acknowledgments

The authors express their gratitude to Dr. Di Wu for his valuable insights on animal brain transplantation, and to Dr. Zhigang Qi for his contributions to imaging examinations and to Mr. Peng Xu for his technical assistance with surgical robotics. The authors are equally grateful to Dr. Yanhui Ma and Mr. Zixin Zhu for their professional expertise in animal anesthesia and physiological monitoring throughout the experimental procedures.

Author Contributions

Z.C. and D.H conceived and supervised the research. D.H. and S.C. performed the brain injection surgery. D.H., X.W., and W.W. performed rat injection. D.H., X.W., W.W., and T.Z. conducted the molecular biology experiments, cell culture, sample collection measurement. D.H. and Z.C. conducted data analysis. D.H. and Z.C. drafted the manuscript. All authors have reviewed the manuscript and approved the submission.

Availability of Data and Material

All data are available in the main text or the Supplementary Materials.

Ethical Approval

This study was approved by our institutional review board.

Statement of Human and Animal Rights

All the experimental procedures were conducted in compliance with the Guidelines for the Care and Use of Laboratory Animals established by the Beijing Association for Laboratory Animal Science and the National Institutes of Health Guide for the Care and Use of Laboratory Animals. All procedures performed in studies involving animals were approved by the Laboratory Animal Ethics Committee of Xuanwu Hospital Capital Medical University.

Statement of Informed Consent

There are no human subjects in this article and informed consent is not applicable.

Declaration of Conflicting Interests

The author(s) declared no potential conflicts of interest with respect to the research, authorship, and/or publication of this article.

Funding

The author(s) disclosed receipt of the following financial support for the research, authorship, and/or publication of this article: This work was supported by the National Natural Science Foundation of China (82171250), Beijing Natural Science Foundation (7242068), the Project for Technology Development of Beijing-affiliated Medical Research Institutes (11000023T000002036310), Beijing Hospitals Authority's Ascent Plan (DFL20240804), Hui Zhi talent project (HZ2021ZCLJ004).

ORCID iDs

Deqiang Han https://orcid.org/0000-0001-8187-0355
Zhiguo Chen https://orcid.org/0000-0003-1508-510X

Supplemental Material

Supplemental material for this article is available online.

References

1. Chen X, Jiang S, Wang R, Bao X, Li Y. Neural stem cells in the treatment of Alzheimer's disease: current status, challenges, and future prospects. *J Alzheimers Dis*. 2023;94(s1):S173–86.
2. Temple S. Advancing cell therapy for neurodegenerative diseases. *Cell Stem Cell*. 2023;30(5):512–29.
3. Parmar M, Grealish S, Henchcliffe C. The future of stem cell therapies for Parkinson disease. *Nat Rev Neurosci*. 2020;21(2):103–15.
4. Rust R, Nih LR, Liberale L, Yin H, El Amki M, Ong LK, Zlokovic BV. Brain repair mechanisms after cell therapy for stroke. *Brain*. 2024:awae204.
5. Schweitzer JS, Song B, Herrington TM, Park T-Y, Lee N, Ko S, Jeon J, Cha Y, Kim K, Li Q, Henchcliffe C, et al. Personalized iPSC-Derived Dopamine Progenitor Cells for Parkinson's Disease. *N Engl J Med*. 2020;382(20):1926–32.
6. Huang H, Bach JR, Sharma HS, Chen L, Wu P, Sarnowska A, Otom A, Xue M, Saberi H, He X, Alhawamdeh Z, et al. The 2023 yearbook of Neurorestoratology. *J Neurorestoratology*. 2024;12:100136.
7. Huang H, Chen L, Sanberg PR, Dimitrijevic M, Shetty AK, Sharma HS, Wu P, Bryukhovetskiy A, Al-Zoubi ZM, Chopp M, Young W, et al. Beijing Declaration of International Association of Neurorestoratology (2023 Xi'an version). *J Neurorestoratology*. 2023;11(2):100055.
8. Xue J, Wu Y, Bao Y, Zhao M, Li F, Sun J, Sun Y, Wang J, Chen L, Mao Y, Schweitzer JS, et al. Clinical considerations in Parkinson's disease cell therapy. *Ageing Res Rev*. 2023;83.
9. Lochhead JJ, Thorne RG. Intranasal delivery of biologics to the central nervous system. *Adv Drug Deliv Rev*. 2012;64(7):614–28.
10. Wang X, Yin Y, Zhou H, Chi B, Guan L, Li P, Li J, Wang Y. Drug delivery pathways to the central nervous system via the brain glymphatic system circumventing the blood-brain barrier. *Exploration*. Epub 2024 Jul 9.
11. Achón Buil B, Tackenberg C, Rust R. Editing a gateway for cell therapy across the blood–brain barrier. *Brain*. 2022;146(3):823–41.
12. Hu Y, Cai P, Zhang H, Adilijiang A, Peng J, Li Y, Che S, Lan F, Liu C. A comparation between frame-based and robot-assisted in stereotactic biopsy. *Front Neurol*. 2022;13:928070.
13. Owen CM, Linskey ME. Frame-based stereotaxy in a frameless era: current capabilities, relative role, and the positive- and negative predictive values of blood through the needle. *J Neurooncol*. 2009;93(1):139–49.
14. Dagnino G, Kundrat D. Robot-assistive minimally invasive surgery: trends and future directions. *Int J Intell Robot Appl*. 2024;8:812–826.
15. Ball T, González-Martínez J, Zemmar A, Sweid A, Chandra S, VanSickle D, Neimat JS, Jabbour P, Wu C. Robotic applications

in cranial neurosurgery: current and future. *Oper Neurosurg*. 2021;21(6):371–79.
16. Wang X, Han D, Zheng T, Ma J, Chen Z. Modulation of human induced neural stem cell-derived dopaminergic neurons by DREADD reveals therapeutic effects on a mouse model of Parkinson's disease. *Stem Cell Res Ther*. 2024;15(1):297.
17. Li C, Wu S, Huang K, Li R, Jiang W, Wang J, Shu K, Lei T. A comparison of the safety, efficacy, and accuracy of frame-based versus remebot robot-assisted stereotactic systems for biopsy of brainstem tumors. *Brain Sci*. 2023;13(2):362.
18. Kondziolka D, Gobbel GT, Fellows-Mayle W, Chang YF, Uram M. Injection parameters affect cell viability and implant volumes in automated cell delivery for the brain. *Cell Transplant*. 2011;20(11-12):1901–1906.
19. Shen WB, Plachez C, Chan A, Yarnell D, Puche AC, Fishman PS, Yarowsky P. Human neural progenitor cells retain viability, phenotype, proliferation, and lineage differentiation when labeled with a novel iron oxide nanoparticle, Molday ION Rhodamine B. *Int J Nanomedicine*. 2013;8:4593–4600.
20. Zheng X, Han D, Liu W, Wang X, Pan N, Wang Y, Chen Z. Human iPSC-derived midbrain organoids functionally integrate into striatum circuits and restore motor function in a mouse model of Parkinson's disease. *Theranostics*. 2023;13(8):2673–92.
21. Yuan Y, Tang X, Bai YF, Wang S, An J, Wu Y, Xu ZD, Zhang YA, Chen Z. Dopaminergic precursors differentiated from human blood-derived induced neural stem cells improve symptoms of a mouse Parkinson's disease model. *Theranostics*. 2018;8(17):4679–94.
22. Chen Z, Zhao G. First-in-human transplantation of autologous induced neural stem cell-derived dopaminergic precursors to treat Parkinson's disease. *Sci Bull*. 2023;68(22): 2700–2703.
23. Potts MB, Silvestrini MT, Lim DA. Devices for cell transplantation into the central nervous system: design considerations and emerging technologies. *Surg Neurol Int*. 2013;4(Suppl 1):S22–30.
24. Janowski M, Lyczek A, Engels C, Xu J, Lukomska B, Bulte JW, Walczak P. Cell size and velocity of injection are major determinants of the safety of intracarotid stem cell transplantation. *J Cereb Blood Flow Metab*. 2013;33(6):921–27.
25. Kawabori M, Tanimori A, Kitta S, Shichinohe H, Houkin K. Evaluation of novel stereotactic cannula for stem cell transplantation against central nervous system disease. *Stem Cells Int*. 2020;2020:4085617.
26. Schweitzer JS, Song B, Leblanc PR, Feitosa M, Carter BS, Kim K-S. Columnar injection for intracerebral cell therapy. *Oper Neurosurg*. 2020;18(3):321–28.